FRACTURE BEHAVIOR OF RIVETED LAP JOINTS DUE TO PROJECTILE IMPACTS

Tomoaki Matsuda*, Koji Mizutani*, Shingo Enomoto*,
Masahiro Nishida, Tomoki Moroe** and Koki Yamada****
*** Churyo Engineering CO., LTD., 10, Oye-cho, Minato-ku, Nagoya 455-8515, Japan,**
**** Nagoya Institute of Technology, Gokiso-cho, Showa-ku, Nagoya 466-8555, Japan,**
to-matsuda@churyo.co.jp
Keywords: *fracture behavior, riveted lap joints, projectile impact, crack, perforation*

Abstract

Through experiments that the projectile collided against structures that simulate aircraft structure, we confirmed fracture behavior around the riveted lap joint parts. We also tried to reproduce the fracture behavior using FE-Analysis. In addition, we discussed the fracture behavior around the riveted lap joint of the structure, based on the results of the experiment and simulations.

1 Introduction

Aircraft structures are made up of the skin, frame, and stringer. These parts are joined together by rivets. During an emergency like a rotor burst or tire burst, if fragments of these parts collide against the riveted lap joint and destroy the parts surrounding the joints, this is highly likely to impair the safety of the aircraft in a devastating manner.

On the other hand, there have been multiple reports concerning the collision phenomenon [1][2][3]. However, most of these reports are results of collision experiments based on single parts like the plate. Such collision research on separate parts alone cannot clarify the sort of fracture behavior that can manifest when collisions occur on lap joints with multiple materials, such as those in actual structures.

Therefore, we implemented collision experiments using a specimen that joins the skin, a stringer, and a frame with rivets. As the projectile, we used a bearing ball (the first experimental consideration) and it collided against the riveted lap joint section of the specimen.

As a result, we were able to observe differences in fracture behavior manifesting on the specimen after collision, based on the difference in the impact position and projectile velocity.

Next, through a simulation using FEM, we reproduced the fracture behavior that was observed during the experiment. We then further discussed the fracture behavior manifesting around the riveted lap joints based on both the experiment and the simulation.

2 Experiment

2.1 Specimens and Experimental Methods

In this study, a spherical projectile made of bearing steel, JIS: SUJ-2, with a diameter of 10.0[mm] was used. As a target, we used a specimen that joined the skin, frame, and stringer (of a simulated aircraft structure) by rivets. Fig.1 shows the appearance and dimensions of the specimen. Furthermore, the materials and thicknesses of its components are shown on Table 1. Two types of rivets, namely NASM20470 (Round) and NASM20426 (Countersunk) were used.

The spherical projectile was accelerated by using a gas gun and impacted to the target [5]. The equipment is shown in Fig.2.

Here, we performed 12 cases of experiments that varied the impact position and projectile velocity.

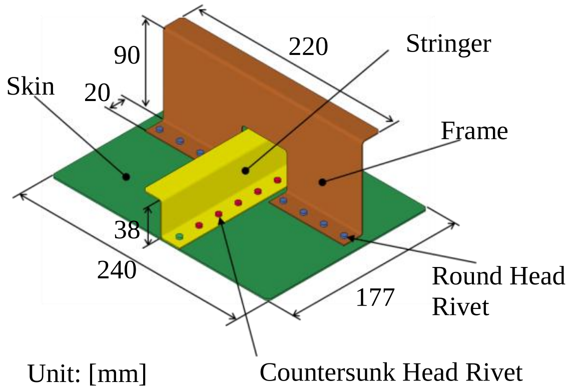

Fig.1 Specimen

Table 1 Material and Thickness

Part	Material	Thickness [mm]
Skin	A2024-T3	1.6
Stringer	A5052-H34	1.0
Frame	A5052-H34	1.0
Countersunk Head Rivet	A2117-T3	-
Round Head Rivet	A2117-T3	-
Spherical Projectile	S45C	-

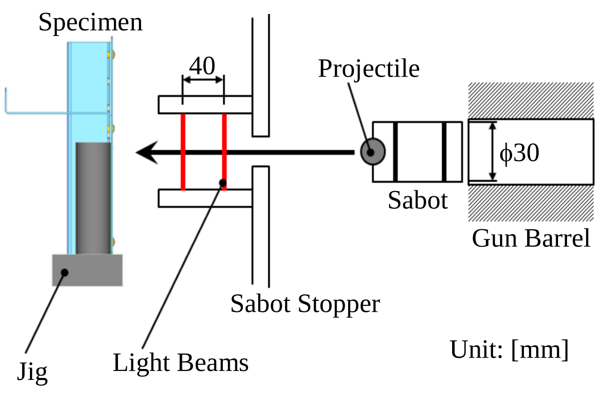

Fig.2 Overview of Equipment

2.2 Experimental Results

For the 12 cases of experiments that were performed, the projectile velocity and the distance between the impact position and the closest rivet are shown in Table 2. The distance denotes the length of distance between the center of impact and the center of the rivet.

The result of impact test case No. 1 is shown in Fig. 3. The shown side is impacted side. This case is the result of velocity: 208.0[m/s], and minimum distance from rivets: 9.2[mm]. Although the skin was perforated in this case, the stringer was not perforated. Furthermore, cracks had formed from the perforation hole in the skin towards the rivet.

The result of impact test case No. 3 is shown in Fig. 4. The shown side is the impacted side. Fig. 4 is the result of velocity: 161.3[m/s], and minimum distance from rivets: 16.8[mm]. In this case, the projectile perforated the skin. No cracks formed from the perforation hole of the skin towards the rivet.

The result of impact test case No.6 is shown in Fig. 5. The shown side is the impacted side. Fig. 5 is the result of velocity: 227.3[m/s], and minimum distance from rivets: 14.7[mm]. In this case, both the skin and the stringer were perforated. Large cracks had formed from the perforation hole of the skin to the No. 1 and No. 2 rivets. Unlike impact test case No. 1, this crack is thought to have formed due to the shearing force in the out-of-place direction from the skin surface. (Please note here, that for the sake of convenience, all linear-shaped fracture patterns are described as “cracks”.)

Table 2 Minimum Distance and Impact Velocity

Case No.	Min. Distance [mm]	Impact Velocity [m/s]
1	9.2	208.0
2	1.1	200.0
3	16.8	161.3
4	10.4	208.3
5	9.1	185.2
6	14.7	227.3
7	8.2	219.3
8	12.5	166.7
9	19.0	174.8
10	7.0	138.9
11	11.5	139.7
12	6.5	151.0

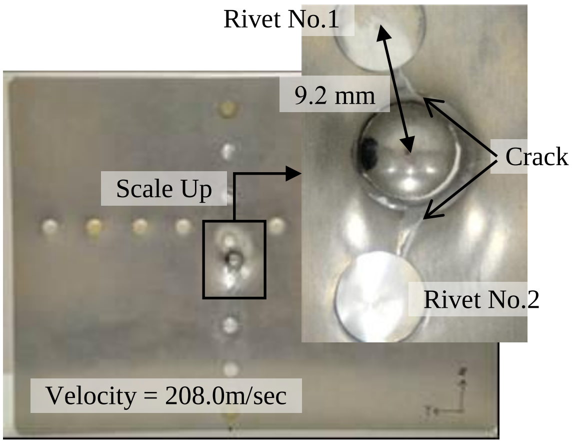

Fig.3 Experimental Result (No.1)

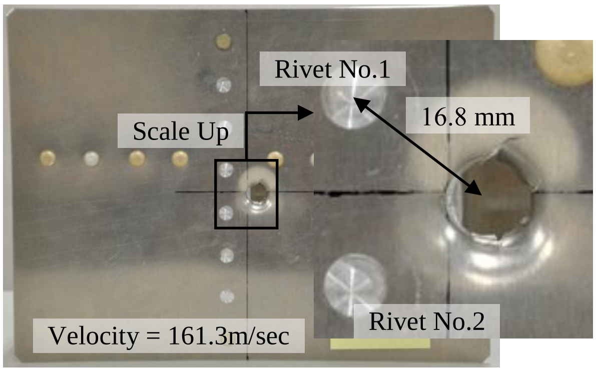

Fig.4 Experimental Result (No.3)

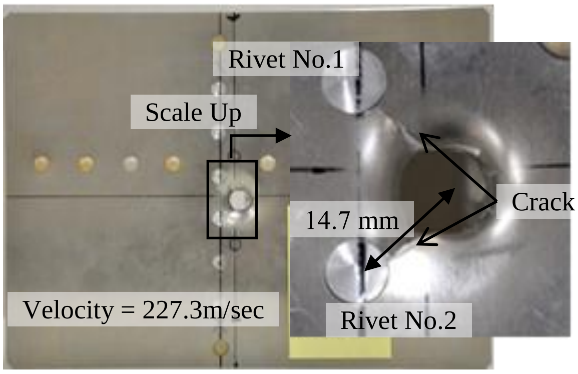

Fig.5 Experimental Result (No.6)

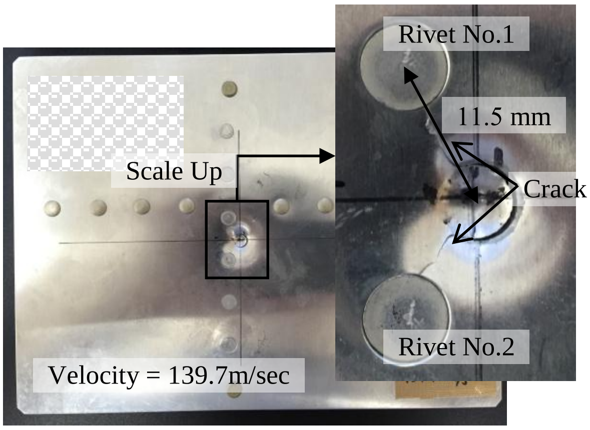

Fig.6 Experimental Result (No.11)

Fig. 6 shows impact test case No. 11. For this case, the minimum distance was 11.5[mm], while the impact velocity was 139.7[m/s]. Despite there not being any perforation for this impact test case, cracks formed towards the rivets.

3 Simulations

3.1 Finite Element Model

We then attempted to reproduce the test results using FE-Analysis. For the FE-Analysis code, we used LS-DYNA, a general-purpose non-linear solving program. All parts (skin, frame, stringer, and rivets) were modeled using solid elements. The hexagon element was used for all solid elements. Fig. 7 shows an overview of the FE model.

We referred to reference [4] for the mesh size and material property data of the FE model. For contact, we used the segment-based contact method and set the coefficients of static and dynamic friction. With respect to the material constitutive law, *MAT_PIECEWISE_LINEAR _PLASTICITY (MAT_024) was used as the aluminum alloy, while *MAT_ELASTIC (MAT_001) was used as steel. To express the fracture, we used element erosion. The fracture was rated as equivalent plastic strain, and based on the fracture strain obtained from the material tensile test using DIC (Digital Image Correlation), we considered the dependence of damage levels on the mesh size.

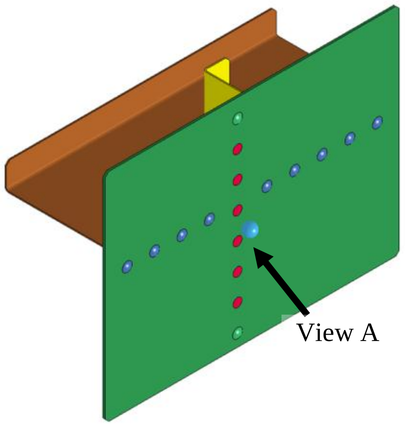

(a) Overview

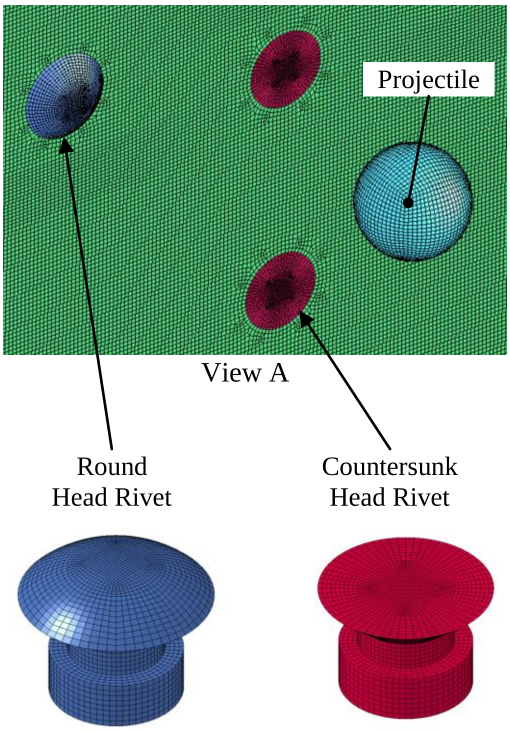

(b) Riveted Lap Joint (view A)

Fig.7 Finite Element Model

3.2 Result

Figs. 8, 9, 10, and 11 show the results of simulations carried out under the same conditions as the experimental results shown in Figs. 3, 4, 5, and 6. As a result of simulations using LS-DYNA, in some of the cases, we were able to reproduce fracture behaviors that were similar to the test results. For example, with respect to the impact test case No. 1 (Fig. 8), it was possible to reproduce the perforation phenomenon (plug) of the skin, as well as the cracks that extend from the perforation hole to the riveted lap joints.

However, with respect to impact test cases No. 6 (Fig. 10) and No. 11 (Fig. 11), it was not possible to simulate the cracks connecting rivets that were seen in the impact tests. This is because this crack formation is a phenomenon that depends not only on the tensile force into the plane due to the impact, but is dominated by the shearing force out of the plane. Furthermore, this is a phenomenon not easily reproduced using the element erosion method, which rated the impact as plastic strain based on the results of uniaxial tensile tests.

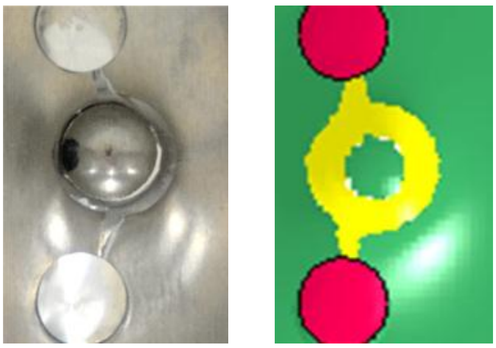

Fig.8 Simulation Result as Same Condition as Impact Test No.1

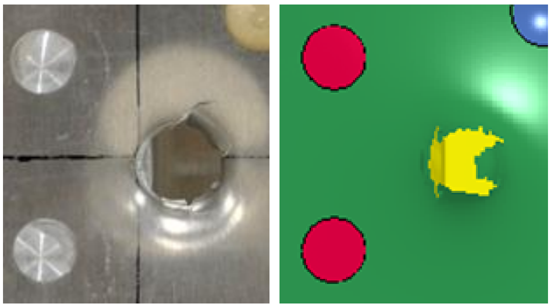

Fig.9 Simulation Result as Same Condition as Impact Test No.3

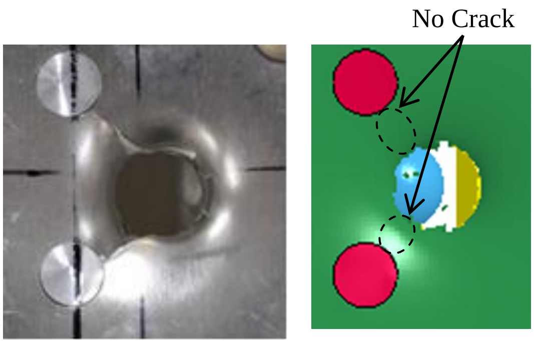

Fig.10 Simulation Result as Same Condition as Impact Test No.6

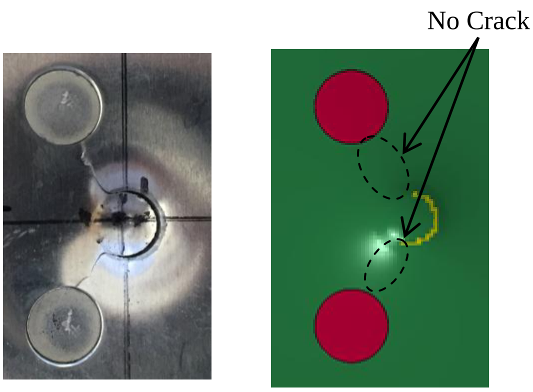

Fig.11 Simulation Result as Same Condition as Impact Test No.11

4 Examination

4.1 Fracture Behavior

Fig. 12 shows a graph of the relationship between the impact velocity and minimum distance that are shown in Table 2. The distance expressed on the horizontal axis denotes the distance between the center of impact and the center of the rivet.

On Fig. 12, test cases that formed cracks between the impact hole and the riveted lap joint are marked with red circles. The black dotted line denotes the total distance obtained by adding the rivet radius to the projectile radius. The blue dotted line denotes the crack formation speed limit (150[m/s]) on simple thin metal plates, as reported in [4]. In addition, the red dotted line has been shown in reference to the permissible limit from reference [6]. (Here, the radius 5.0[mm] of the projectile has been added to the minimum permissible distance 12.7[mm] from the damaged part to the fastener row.)

Regions “A, B, C” in Fig. 12 show the difference in impact the projectile can have on the riveted lap joint, as discovered from the test results. “A” is a region where the projectile collides directly with the rivet. In regions “B” and “C”, cracks connecting the impact site to the riveted lap joint form. Region “B” was reproducible through simulation. Cases in “C” formed cracks in out-of-plane direction and cannot be simulated as of yet.

In region “D”, there are cases for which cracks connecting to the rivets were not observed.

Table 3 summarizes the difference in fracture behavior by minimum distance and the results of simulations.

When looking at Fig. 12, the distance of permissible limit shown in reference [6] and the distance of crack formation as obtained from the results of this test seem to have a correlation.

When focusing on the impact test case No. 11 that falls within region “C,” despite the projectile not perforating through, cracks joining the impact site to the riveted lap joint form for this case.

The following observations were gained from the results of this test. That is, with respect to assessing the safety after the impact, while a simple thin metal plate would only tell whether there would be perforation or not, riveted lap joint structures not only provide information about the perforation but also about the possibility of crack formations that connect to the riveted lap joints.

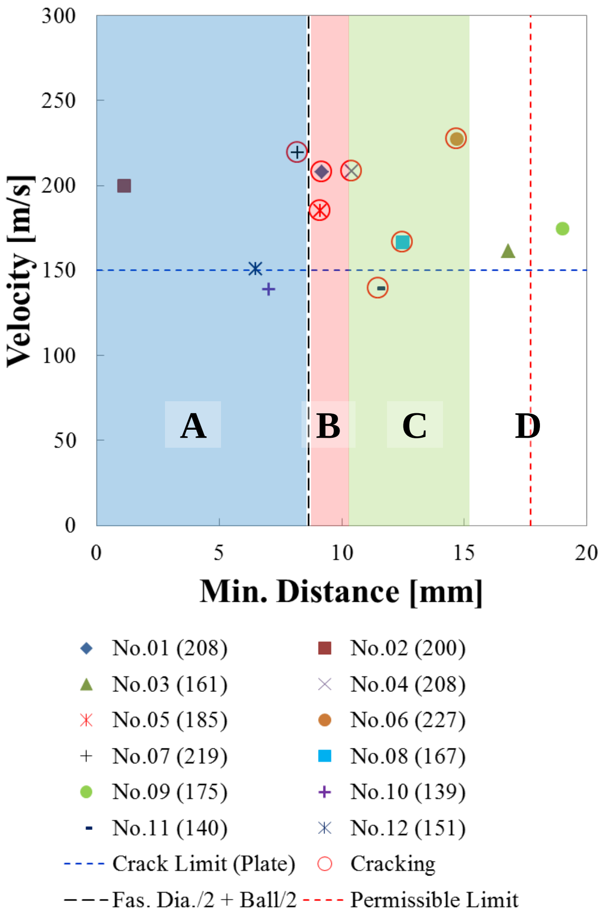

Fig.12 Min. Distance vs. Impact Velocity

Table 3 Fracture Behavior

Pattern	Fracture Behavior	Simulation
A	Impact to Rivet	OK
B	Crack toward Rivet	OK
C	Crack toward Rivet (out-of-plane shearing)	Impossible
D	Perforation and No Crack toward Rivet	OK

4.2 Difference with Plate

Although results of impact tests using simple thin metal plates have been reported in [1][2][3], etc., with such thin plates, despite crack formations around the centers of impact, the cracks do not seem to manifest in a specific direction.

On the other hand, as shown in Figs. 3, 5, and 6, in this test the cracks had formed from the impact site towards the rivets. However, at a certain impact velocity, when the minimum distance falls within region “D” of Fig.12, cracks towards the rivets stop forming. Because of this, it is clear that different fracture behaviors from thin plates form only around the riveted lap joints.

In order to clarify whether this is the impact of the rivets themselves, or the impact of the rivet holes, we carried out a test using a thin plate specimen with holes for rivets.

The rivet hole had a diameter of 4 [mm], and the projectile was targeted to a position that is 12.2[mm] away from the center of the rivet hole, at a velocity of 143.7[m/s]. The test results are shown in Fig. 13. As a result, despite the projectile making impact near the hole, the crack did not progress towards the hole. Instead, such as when the projectiles collided against the thin plate, cracks formed regardless of the hole. For this reason, it is conceivable that cracks directed towards riveted lap joints form, not simply due to the influence of the holes, but because multiple materials are being joined by rivets.

Fig.13 Thin-Plate with Circular Experimental Result

5 Conclusions

(1) Bearing balls were targeted at specimens that simulated aircraft structures, and their fracture behavior was confirmed.
(2) Using FE-Analysis, simulations were carried out under the same conditions as the test. As a result, although some of the test results were reproducible through simulation, there were some phenomena that could not be reproduced. Future challenges involve FE-Analysis modelling for reproducing all test results.
(3) After confirming the fracture behavior around the riveted lap joint, we discovered the need to consider the effect of cracks that run from the perforation site to the rivets to assess safety, rather than simply assessing the presence or absence of perforation.
(4) With respect to the fracture behavior, we sorted the test results and simulation results by the relationship between the impact velocity and the minimum distance. As a result, we were able to classify the fracture behaviors where the projectile made impact with the riveted lap joint.
(5) We learned that the boundary for crack formations that impact the riveted lap joint segment was within 14.7[mm] to 16.8[mm] of a minimum distance from rivet.
(6) In future, we will add more test cases while establishing a FE-Analysis method that can reproduce the test results. Furthermore, we will consider the difference in plate thickness, rivet sizes, and materials, from both testing and analytical perspectives. Ultimately, we aim to formulate a system for safety assessments whenever projectiles make impact with segments surrounding the riveted lap joint.

References

[1] Tanaka K, Kurokawa T, Yoneda H and Adachi K. Thin metallic plate perforation. *Journal of the Japan Society for Aeronautical and Space Sciences*, Vol. 33, No. 379, pp 38-45, 1985.

[2] Kawano S, Kaminishi K, Yamashita M and Shimizu S. Study on penetration of ductile thin metal plate (1st report, total work done for thin metal plate during quasi-static penetration by conical punch). *Transactions of the Japan Society of Mechanical Engineers Series A* Vol. 53, No. 491, pp 1307-1315, 1987.

[3] Kawanishi K, Kawano S, Nanba T and Taneda M. Study on penetration of thin metal plate (2nd report, dependence of energy-absorbing capacity on the mechanical properties). *Transactions of the Japan Society of Mechanical Engineers Series A*, Vol. 55, No. 515, pp 1601-1606, 1989.

[4] Yamada K, Moroe T, Nishida M, Mizutani K, Enomoto S, Matsuda T, Bae K-O and Shin H-S. Finite element simulation and experiment studies on projectile perforation of circular and rectangular plates. *Proc ISIE (International Symposium on Impact Engineering) 2016*.

[5] Nishida M, Tanaka K, Experimental study of perforation and cracking of water-filled aluminum tubes impacted by steel spheres. *Int. J. Impact Eng.* Vol. 32 , pp 2000-2016, 2006.

[6] Michael Chun-Yung Niu, *Airframe Stress Analysis and Sizing.* 2nd edition, Hong Kong Conmilit Press LTD, 1999.

Contact Author Email Address

mailto : to-matsuda@churyo.co.jp

Copyright Statement